Production of Microporous Resins for Heavy-Metal Removal. II. Functionalized Polymers

Judith Cardoso,[1] Jesús Ortiz-Palacios,[1] Octavio Manero[2]

[1]*Departamento de Física, Ciencias Básicas e Ingeniena, Universidad Autónoma Metropolitana-Iztapalape, UAM-I, Apartado Postal 55-534, México DF 09340, México*
[2]*Instituto de Investigaciones en Materiales, Universidad Nacional Autónoma de México, Apartado Postal 70-360, México DF 04510, México*

Received 4 January 2007; accepted 30 September 2007
DOI 10.1002/app.27422
Published online 5 December 2007 in Wiley InterScience (www.interscience.wiley.com).

ABSTRACT: Ion-exchange polymers were used successfully in water-treatment operations. In this study, three ion-exchange resins based on 4-vinylpyridine and divinylbenzene functionalized with *N*-oxide groups were obtained. Their ion-adsorption properties were measured in solutions containing chromium at concentrations of 4 and 500 ppm with column and batch equilibrium techniques. The removal efficiency of the chromium ions with HCl was observed to increase after the protonation of the *N*-oxide groups. The resins could be reused after 10 cycles with the metal removal efficiency maintained at higher than 95%. These studies evidenced a strong correlation between the morphology and ionic group content in the resin and its chromium ion sorption capability. © 2007 Wiley Periodicals, Inc. J Appl Polym Sci 107: 3644–3653, 2008

Key words: adsorption; functionalization of polymers; morphology; resins; ion exchangers

INTRODUCTION

The hazardous effects of heavy metals in nature have considerably limited their use in industry. With our ever-increasing population and rapid industrial growth, environmental pollution is also produced by metal discharge from various industries. Toxic metal-ion removal requires an ion-exchange reaction for the complexation of cations or anions through electrostatic binding. Ion-exchange resins are suitable for metal-ion complexation because of their hydrophobicity and high selectivity.[1,2] The synthesis of a polymer for these applications, therefore, requires specific functionalization to improve the sorption capabilities of the resin. Synthetic ion exchangers have become widely used in both industry and academia for separation operations of inorganic and organic ions. Among the most popular precursor copolymers for obtaining ion exchangers with different functionalities and morphologies are styrene (St)–divinylbenzene (DVB) copolymers. Functional copolymers, linear and crosslinked, bearing primary amine groups are of great interest because of their high reactivity, which allows the incorporation of numerous additional moieties.[3] However, ion exchangers with primary amine groups are difficult to obtain by chemical reactions with St–DVB copolymers.

Correspondence to: J. Cardoso (jcam@xanum.uam.mx).

Journal of Applied Polymer Science, Vol. 107, 3644–3653 (2008)

The removal of Cr(VI) in wastewater is of significant importance from an environmental viewpoint. Conventional methods for the removal of Cr(VI) include chemical precipitation, redox reactions, mechanical filtration, membrane separation, ion exchange, and adsorption.[4–7] Chromium ion content should be less than 0.05 mg/L for permissible levels.[8] In general, Cr(VI) exists in aqueous solutions as oxyanions. Below pH 6, hexavalent chromium is found primarily as hydrogen chromate ion ($HCrO_4^-$) and dichromate ion ($Cr_2O_7^{-2}$). Above pH 6, the chromate ion (CrO_4^{-2}) becomes the dominant species. Because these ions are carcinogenic, mutagenic, and teratogenic through dermal and oral exposure, they can be major pollutants in the waste streams from these industries.[9,10]

Adsorption has been one of the methods used to remove chromium species and toxic metals from aqueous solutions containing relatively low ion concentrations. There are many types of adsorbents, including activated carbon,[11–15]carbon slurries,[16] biomaterials,[17,18] chitosan,[19] sawdust,[20] polyacrylamide-grafted sawdust,[21] polyacrylonitrile fibers,[22] modified poly(4-vinylpyridine) [poly(4VP)] coated gels,[23] poly(4VP),[24] and 4-vinyl pyridine grafted poly(ethylene terephthalate),[25] that have been studied for the adsorption of chromium from aqueous solutions. However, some of these adsorbents do not have high adsorption capacities or need long adsorption equilibrium times, whereas others may have difficulty in regeneration and reuse. One of the recent

developments in the removal of heavy-metal ions from water or wastewater is the use of polymer beads as adsorbents. This is mainly attributed to the relatively large external specific high surface areas, high adsorption kinetics, and relatively low cost of these polymer beads.[26,27] Anion-exchange resins made from St–DVB present good removal capabilities at pH 3–4, whereas within the alkaline or neutral pH range, their removal capabilities decrease drastically.[28]

Data on the binding of amines and other bases to metal ions are available. In a study by Rivas et al.,[29] the percentage retention in batch equilibrium tests for various metal ions (Cd^{+2}, Cu^{+2}, Cr^{+3}, Hg^{+2}, Pb^{+2}, U^{+6}, and Zn^{+2}) was a function of pH and depended on the initial ion concentration. It was observed that as pH increased, more stable complexes were formed among the ions and the polymers.

Neagu et al.[30] synthesized strong-base anionic (SBA) exchange resins with aliphatic-functionalized 4-vinylpyridine (4VP)–DVB copolymers. With methyl, ethyl, and butyl aliphatic groups, the adsorption capacity of chromium increased specially with the methyl groups in the polymer matrix.

Previous studies have only reported chromium removal for concentrations less than or equal to 100 mg/L and for pH values lower than 5. The values reported have varied in the range 1.4–91 mg/g for the adsorption capacities of chromium[29–32] with the range where the adsorption capacity of poly(4VP) beads is observed. Thus, this polymer represents an interesting alternative as an industrial adsorbent.

Recently, suspension polymerization was used to produce adsorption resins with various morphologies and generate microporous structures in organic solvents or their mixtures (porogens).[33] Resins were produced with various morphologies and large surface areas from 4VP and DVB comonomers, and their sorption capabilities for heavy-metal ions were tested. This study was reported in part I of this study.[34]

On the other hand, special attention has been given to the preparation of zwitterionic polymers because of their applications as surfactant and antistatic agents in biomedical devices and in membranes of high selectivity.[35–37] These compounds are also recognized as bipolar ions or inner salts. Because of their ability to form polymer–metal complexes, they can be used for metal extractions. In particular, the *N*-oxide zwitterionic polymers have potential in biological applications because they can act as electron donors or electron acceptors.[37] The incorporation of these functional groups into a resin may turn from cationic (for pH < 6.5) to an ampholytic (for pH $= 6.5$ at the isoelectric point) and to anionic (for pH > 6.5).[38]

The objective of this study was the synthesis of porous resins of the gel type with large surface areas, to incorporate the *N*-oxide groups in the same resins produced in part I of this study, for heavy-metal-ion removal. In particular, in this study, we focused on the assessment of the ion-exchange properties of the porous resins for applications concerning ion removal (Cr^{+6}) in water-treatment operations.

EXPERIMENTAL

Material synthesis

The functionalized resins ware obtained from the same precursor polymers used to produce macroporous resins, which were synthesized in suspension from the 4VP–DVB precursor, poly(vinyl alcohol), and an organic solvent as a porogen agent. The resulting materials were labeled PM40, PM20, and PM10 and had monomer proportions (4VP : DVB) of 60 : 40, 80 : 20, and 90 : 10 mol, respectively.[34] The following procedure used for the functionalization reactions was carried out.[38] In a reactor vessel provided with a magnetic stirrer, thermometer, reflux condenser, and nitrogen inlet valve, the precursor resins (PM10, PM20, and PM40) were added with acetic acid. Subsequently, the mixture was heated to 80°C, and hydrogen peroxide was added in two parts. An amount corresponding to an equivalent of the pyridinic group was initially added, and another 0.3 equiv was added after 3 h. The reaction completion time amounted to 18 h. The precursor resin showed a white color, whereas the functionalized resin had a light yellow color. The acetic acid excess was eliminated through various deionized water washings to a pH of 6. Azeotropic distillation was used to eliminate the residual acetic acid. The material was then dried in a vacuum oven at 50°C for 48 h.

Polymer characterization

Polymer characterization was carried out with Fourier transform infrared (FTIR) spectroscopy (Perkin-Elmer, Spectrum GX) (Norwalk, CT), elemental analysis (PerkinElmer) (Norwalk, CT), thermogravimetry (PerkinElmer Pyris) (Norwalk, CT), scanning electron microscopy (Zeiss DSM 940) (Vertrieb, Deutschland), and nitrogen adsorption (Quantachrome Autosorb-1 apparatus) (Boynton Beach, FL). The specific surface areas were calculated from the nitrogen adsorption–desorption isotherms with the Brunauer–Emmett–Teller model.

Measurements of the swelling properties

The copolymers were dissolved in water at ambient temperature to reach equilibrium conditions. After treatment, excess water was removed. The swelling amount (Q) was calculated according to

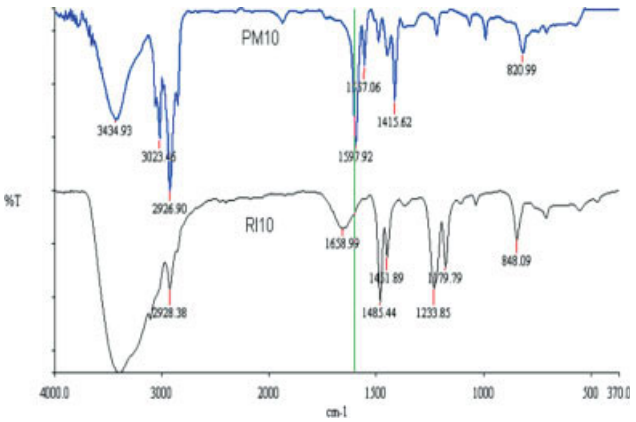

Figure 1 FTIR spectra of the precursor copolymer (PM10) and functionalized copolymer (RI10). [Color figure can be viewed in the online issue, which is available at www.interscience.wiley.com.]

$$Q = (W_s - W_d)/W_d$$

where W_s and W_d are the weights of the swollen and dried copolymers, respectively.

Assessment of the sorption capabilities of the polymers

The sorption capabilities of the polymers were tested in three stages. In the first one, the batch equilibrium technique was carried out under the same conditions described elsewhere.[34] The second stage included the column method, in which 0.5 g of resin was packed in a 50-mL burette. $K_2Cr_2O_7$ solution (40 mL, 4 ppm) was added, and measurements were taken at the burette exit. The pH of the solution was fixed at 6.5. Once the column studies were completed, the resin with the higher retention capability (q) with specific counterions was consider for the regeneration procedure with 5% NaCl solution. The last stage dealt with the evaluation of the sorption capability of the polymer with, once again, the column technique but with a 500-ppm $K_2Cr_2O_7$ solution. Two 50-mL burettes were packed with 1 g of dry resin. To the first one, a 1*M* HCl solution was added, whereas a 5% NaCl solution was added to the second burette. Cr^{6+} was then quantified with the UV–visible spectroscopic technique. The determination of Cr^{+6} ions was carried out in a PerkinElmer Spectrum Lambda 40 with a 540-nm wavelength.[39]

RESULTS AND DISCUSSION

In Figure 1, the FTIR spectra of the precursor (PM10) and functionalized polymers (RI10) with 10% crosslinking are shown. Additional materials produced

TABLE I
Elemental Analysis of the Functionalized Copolymers

Functionalized polymer	Elemental analysis (%)											
	N		C		H		N		O			
	Incorporated[a]	Calculated[b]	Experimental	Theoretical	Experimental	Theoretical	Experimental	Theoretical	Experimental	Theoretical
RI10	81.6	90	61.4	61.8	7.0	6.8	7.7	8.7	22.9	22.7
RI20	67.2	80	64.1	65.2	7.0	6.8	6.2	7.6	21.3	20.4
RI40	41.2	60	71.3	75.8	7.3	7.0	4.1	5.2	17.3	12.0

[a] Nitrogen incorporated into the chain.
[b] Nitrogen calculated from the reaction stoichiometry.

TABLE II
Water and Acetic Acid Contents Calculated from the Elemental Analysis of the Functionalized Copolymers and *Q* Values

Functionalized copolymer	Remaining CH_3COOH (mol)	H_2O/pyridinic groups (mol)	Functionalization (%)	*Q* (%)
RI10	0.02	1.38	96.4	387
RI20	0.36	0.75	80.8	332
RI40	0.05	0.98	89.9	292

with various crosslinking percentages had similar patterns (not shown). The bands at 3023 and 1598 cm^{-1} were assigned to the =C—H stretching band and the aromatic C=C stretching vibration of the precursor polymer (PM10). A wide band at 3434 cm^{-1} detected the presence of water in accordance with thermogravimetric analysis data of the functionalized polymer, due to the O—H bond stretching band in the H_2O molecule. The presence of hydrated water overshadowed the stretching vibration bands of the methyl and methylene groups, which were absent in the precursor polymer. The band at 1659 cm^{-1} corresponded to the —C=N aromatic groups, which was shifted because of the presence of the *N*-oxide groups. The *N*-oxide group had two characteristic stretching bands at 1233 and 848 cm^{-1}. Both were well-resolved bands, because these vibrations were accompanied by a large change in the dipole moment and polarizability.[37,40,41]

Elemental analysis results corrected for the presence of pyridine groups in the precursor polymers are summarized in Table I. These data were in agreement with the stoichiometry implied in the precursor copolymers. According to data disclosed in Table I, up a 96% functionalization of the pyridine nitrogen was obtained after corrections for the water content and remaining acetic acid. These results reflect the high oxidation properties of the reactants (H_2O_2/AcOH), which may have also induced the degradation of the polymer chain, as discussed elsewhere.[42] Elemental analysis data allowed us to calculate the acetic acid amount remaining in the sample and the oxidation degree of the pyridine group (see Table II). Additionally, in Table I, the *Q* values of the synthesized copolymers are disclosed, with the larger value corresponding to the sample RI10, due to its larger *N*-oxide content and morphology features (discussed later). A larger adsorption capacity was expected in this case.

Table III summarizes the thermogravimetric data. Decomposition temperatures decreased upon resin functionalization compared to those of the precursor polymers. The adsorbed amount of water increased up to 19% because of the N—O group content of the polymer. The polymers showed two decomposition stages, which were assigned to the lower thermal stability of the functionalized polymers compared to those of the precursor ones (which were as high as a 55°C difference). Stage I corresponded to a loss of oxygen and water associated with the *N*-oxide group. Water molecules were dissociated, which neutralized the *N*-oxide groups, because of the high dipolar moment of the ionic groups. Elimination of the oxygen of the *N*-oxide group also released the water molecules, as observed in the experimental data. The last stage was similar to that of the precursor polymers, that is, the decomposition of the polymer chains. The decomposition temperature of the second stage depended on the DVB content, and it was lower than that of the precursor polymers, up to 78°C. This difference may have been due to the breakage of the chains during the oxidation stage, which reduced the molecular weight and enhanced their temperature dependence.

Figure 2 presents the micrographs of the precursor and of their functionalized resins. The microporous resin PM40, containing 40% crosslinking agent (DVB) and pure toluene as a porogen agent, showed the largest surface area (130 m^2/g) with spherical domains and a uniform size of 68 μm.[34] In contrast,

TABLE III
Thermal Stabilities of the Synthesized Materials

Polymer	Water (%)	Initial decomposition temperature (°C)	Mass loss (%)	Final decomposition temperature (°C)	Final mass loss (%)
PM10	5	273	6	412	7
PM20	2	283	4	419	19
PM40	5	290	8	426	17
RI10	19	230	20	334	47
RI20	16	228	17	387	40
RI40	7	236	16	407	42

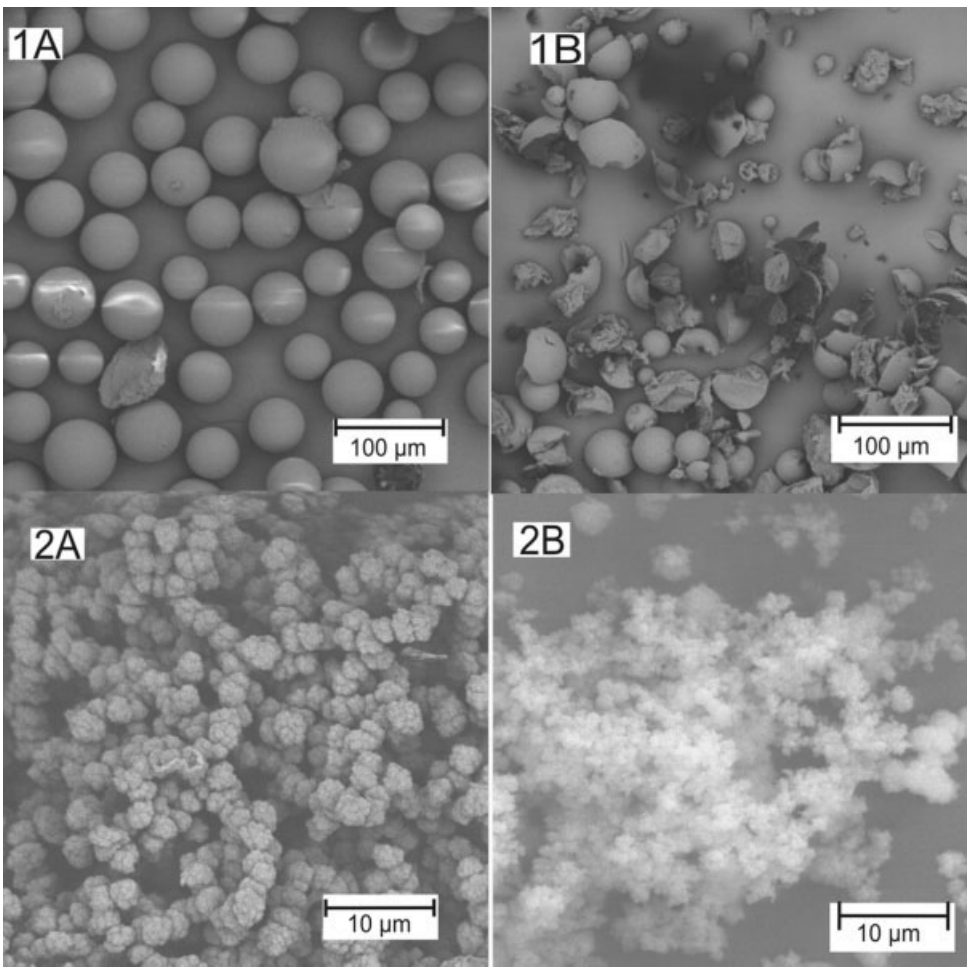

Figure 2 Micrographs of the (1A) precursor (PM40) and (1B) functionalized resins (RI40) with 40% crosslinking (200×) and the (2A) precursor (PM10) and (2B) functionalized resins (RI10) with 10% crosslinking (2000×).

for RI40, the oxidation reaction apparently fractured the original spherical shape. With other toluene/hexane ratios, a microgel (40 : 60) and a gel-type microporous morphology (100 : 0) were observed for PM10 and PM20, respectively. The functionalized resin RI20 depicted a lamellar structure associated with a gel-like structure, and RI10 showed domains resembling aggregated particles of porous lamellar shapes. The nitrogen absorption tests of the RI40 sample showed an isotherm (see Fig. 3) with hysteresis associated with type-IV behavior (according to the IUPAC classification).[43] Type-IV isotherms are characteristic of mesoporous solids containing lamellar-shaped aggregated particles, with stripe-shaped porous structures. The microstripes provide a larger surface area than a smooth surface and lead to a higher adsorption capability. The adsorption takes place in the porous walls similarly to the usual adsorption observed in these kinds of mesoporous structures.[43] They present an increase in the adsorbed compound at relatively intermediate pressures by a multilayer filling mechanism.[44] The surface area of the copolymer is strongly affected by the functionalization reaction. This drastic change was not expected because, according to the current literature, in similar systems, a small change (ca. 5%) was detected in St–DVB copolymers upon functionalization.[29]

Adsorption experiments

Low Cr^{+6} ion concentration

The results in Figure 4 illustrate the adsorption capabilities of the functionalized resins by the plot of q (mg of Cr/g of resin) with time at an initial concentration of 4 ppm with a pH of 6.5. Resin RI20 kinetic data show a q that peaked at 50 h. A small desorption was then observed followed by another increase at longer times. This experiment was repeated to ensure the quality of data. Resins RI10 and RI40 showed a monotonic increase of their q values with time and with RI10 attaining saturation at longer times, mainly because of the reduced number of protonated *N*-oxide groups. With regard to their

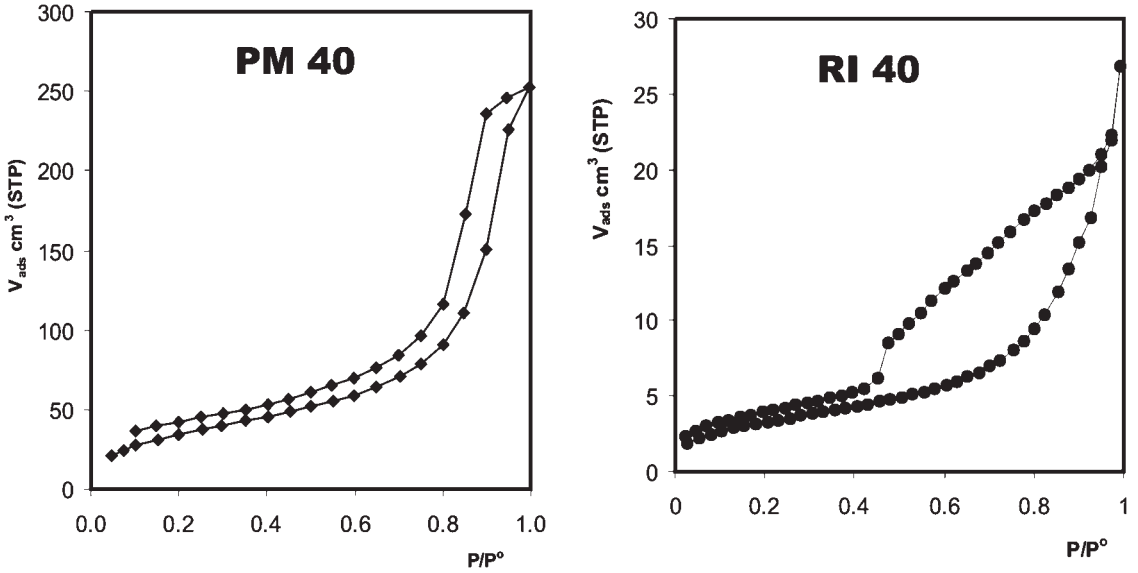

Figure 3 Nitrogen adsorption test of the precursor (PM10) and the functionalized resins (RI40). P and P° are the equilibrium and the saturation pressure of adsorbates and V_{ads} is the adsorbed gas quantity.

morphology, RI40 data show that the sorption capability was not affected by the broken spheres morphology. RI20 depicted a lamellar structure associated with a gel-like structure, in accordance with the micrographs already presented, in which the initial part of the curve detected a slower diffusion time of the particles. The shape of the curve also showed that the material swelled with time, which affected ionic interactions, made the nitrogen–CrO_4^{-2} interaction weaker, and induced a possible desorption. As observed, the q value of the ion-exchange resins depended strongly on the amount of ionic groups present in the polymeric matrix and on their morphological features.

To explain the observed behavior of Cr(VI) adsorption at a pH of 6.5, we needed to examine various mechanisms such as electrostatic interaction and ion exchange, which were responsible for the adsorption on the sorbent surface. At low pH, acid chromate ions ($HCrO_4^{-1}$) were the dominant species, whereas chromates (CrO_4^{-2}) became the main species in solution at pH values of 7.0 and above. For the adsorption of Cr(VI) species on the RI10 beads at pH 6.5, some of the *N*-oxide groups were protonated, and the nitrogen acquired a positive electric charge. The protonated *N*-oxide nitrogens could, therefore, attract the Cr(VI) species, which carried negative electric charges in the solution. Compared to the precursor polymers at pH values around 6.5, the protonation of the pyridine nitrogen of the poly(4VP) beads was probably insignificant, and the electrostatic interaction did not play an important role in the adsorption of Cr(VI) on the sorbent. Similar adsorption mechanisms of hexavalent chromium species on aminated polyacrylonitrile fibers were proposed by Deng and Bai.[22] Because these tests were made with polymers in which the *N*-oxide groups were not fully neutralized, they could be considered adsorption resins under these conditions. Physical adsorption occurred when the *N*-oxide group was not neutralized. On the other hand, ionic interchange resin production implied previous neutralization with HCl or NaCl.

The effect of the initial Cr(VI) concentration on the adsorption efficiency by the RI10 resin was systematically investigated by variation of the initial

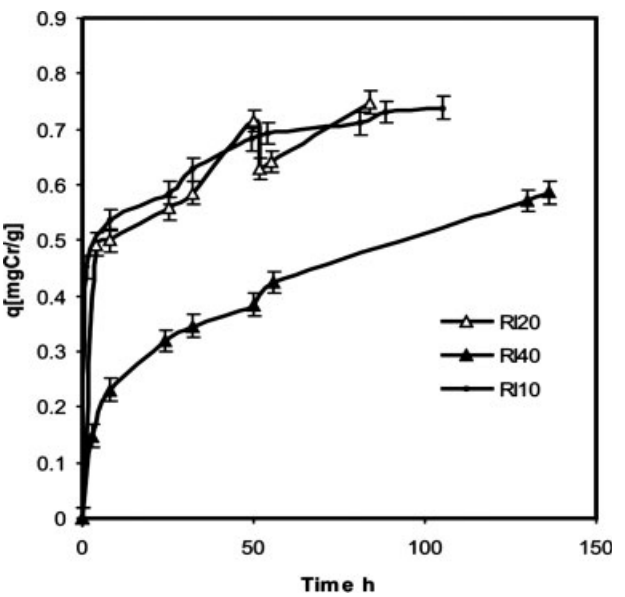

Figure 4 Relationship between the adsorption time and adsorbed amount of Cr(VI) with the functionalized resins in batch (Co = 4 ppm, pH = 6.5, temperature = 298 K).

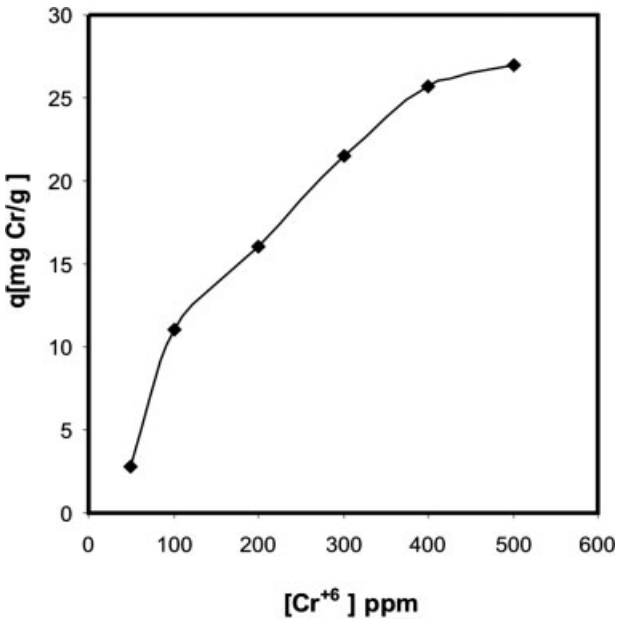

Figure 5 Effect of the initial concentration of Cr(VI) on the adsorption of the functionalized resins (pH = 6.5, temperature = 298 K).

concentration between 50 and 500 mg/L. Figure 5 shows the adsorption results, with the adsorbed mass q (mg Cr/g of resin) and the initial metal concentration at pH 6.5 and 25°C plotted. As shown in this figure, the asymptotic nature of the curve shows that at a higher adsorbate concentration, a saturation limit of the RI10 resin was observed; that is, as the initial metal concentration approached a high value, q_e approached complete monolayer formation. The adsorption isotherms in Figure 5 tended to define a plateau; therefore, it seemed reasonable to suppose that for the experimental conditions used, the formation of a complete monolayer of Cr(VI) ions covering the adsorbent was possible, and the curves led to a constant value of the equilibrium adsorption capability (q_e). The q_e value was 26.9 mg of Cr/g of resin. Its value was twice that obtained for the precursor resin (PM10).[34] Usually, at high adsorbate concentrations, q tended toward the maximum adsorption capability (q_m). Therefore, q_m must have been close to this value.

Column method

The batch equilibrium method led to uncertainties in the exchange capability data, especially when the solution and resin attained ionic equilibrium. For this reason, additional studies in the column were also performed. Figure 6 shows q data as a function of the number of cycles (total effluent volume exiting the column). Resin RI10 presented the largest q value for the chromate ions (CrO_4^{-2}), growing steeply and attaining saturation within four cycles. RI20 and RI40 showed similar trends, growing in a steplike form and leveling off after five cycles. RI20 presented a slight desorption of the ions for longer times, as in the batch tests. This confirmed the assumption made on the strong ionic interactions with the N—O group, although the effect of the resin morphology was also important. RI10 had a larger ionic content, and hence, its q was large in the first cycle, although the magnitude of its specific surface area was not large. On the other hand, RI40 had a lower ionic content, and hence, its q was low in the first cycle, although it had a large specific surface area.

Ion-exchange capability and regeneration of the resins

The resin regeneration and ion recovery procedures involved a particular counterion that the polymer matrix should have contained. The column was prepared as indicated in the Experimental section, with the resin with *N*-oxide groups containing no counterions. A 5% NaCl solution was passed through one burette, while a 1*M* HCl solution was placed in the other burette, and a 4 ppm dichromate solution was prepared. This procedure was intended to provide various counterions to neutralize the *N*-oxide charges. In contrast to previous studies, in this case, at the end of each cycle, the resin was regenerated with the 5% NaCl solution, and this procedure was followed for 10 consecutive cycles. Figure 7 presents the resin q values with various oxygen counterions as a function of the number of cycles.

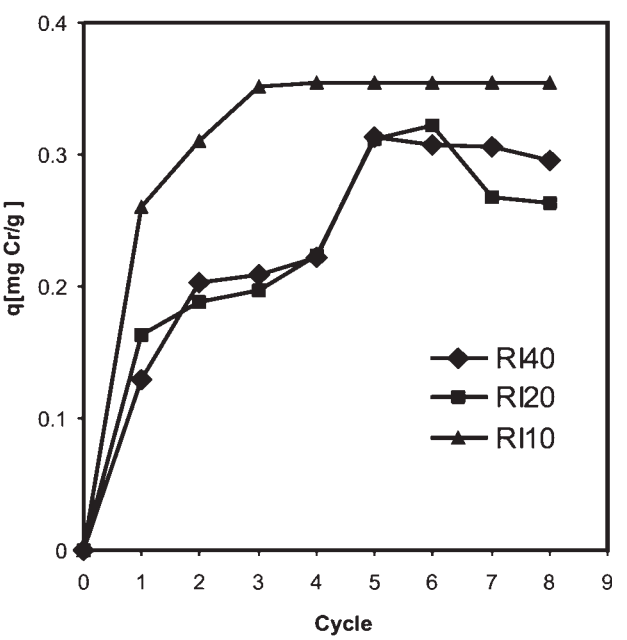

Figure 6 Sorption capability in the column as a function of the number of cycles for the functionalized resins (Co = 4 ppm, pH = 6.5).

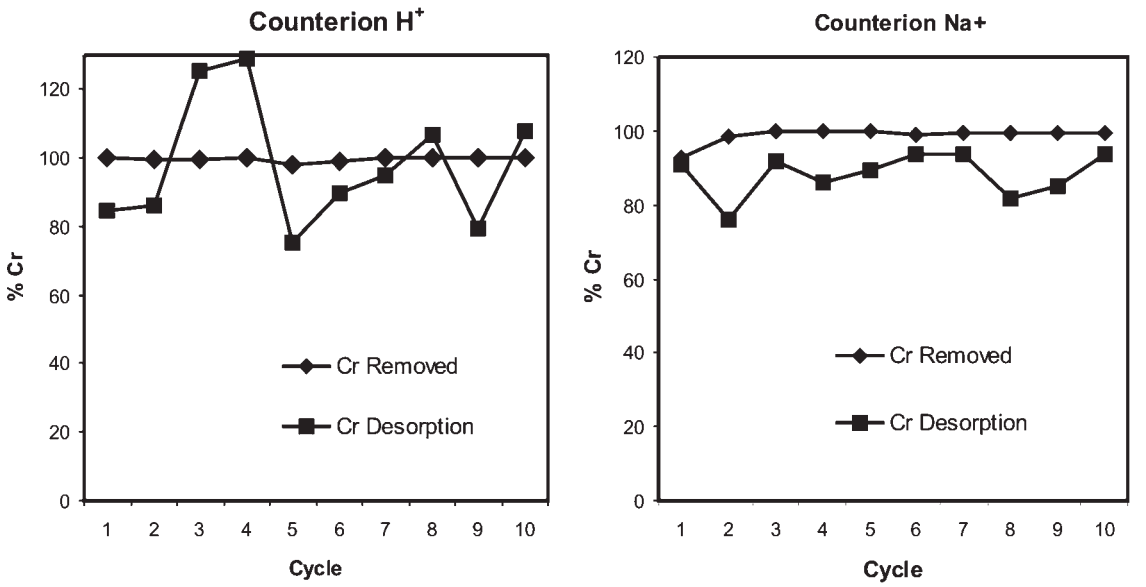

Figure 7 Sorption capability of the RI10 resin with two oxygen counterions as a function of the number of cycles (Co = 4 ppm, pH = 6.5). The study of Cr^{+6} ion desorption is also shown.

As shown in Figure 7, the removal capability for the chromate ions increased in the presence of counterions. In the first cycle, the column containing HCl presented a slightly larger chromate ion removal capability than that observed in the column containing NaCl. During the second cycle, both columns showed a leveling off and achieved a constant removal capability for the remaining cycles. Although the column containing HCl fully eliminated the chromate ions in the solution, it is important to note that the resins must also have eliminated the monovalent $HCrO_4^{-1}$ ions. To explain the observed behavior of Cr^{+6} adsorption with HCl presence, it is necessary to examine the ion-exchange mechanisms. From the stability diagram for the Cr^{+6}–H_2O system, it was evident that at low pH, acid chromate ions ($HCrO_4^-$) were the dominant species. Because the *N*-oxide group is one of the best proton acceptors, its neutralization with HCl generated a covalent hydrogen–oxygen bond (hydroxyl group) joined to the pyridine nitrogen. The induced positive charge on the nitrogen could, therefore, attract the Cr^{+6} species, mainly negatively charged acid chromate ions ($HCrO_4^-$), through electrostatic interaction and ionic exchange with the chloride group (see Fig. 8). Neutralization with NaCl implied a sole electrostatic attraction of the sodium ion with the *N*-oxide group, and therefore, the negative charge of the oxygen prevented further interaction with the $HCrO_4^-$ ions. Although the elimination of chromate ions was not complete in the column containing NaCl, this value fell within limits imposed by the Mexican norm (NOM-127-SSA1) that established a 0.5-ppm limit for Cr^{+6} ion content for human use.

A study of the desorption of Cr^{+6} ions was carried out, and the results are also represented in Figure 7. The Cr^{+6} ions were easily desorbed by treatment of the adsorbent with NaCl. No relevant results were obtained for the desorption process in the acidic solutions. At room temperature ($\sim 25^\circ C$) within 30 min, a desorption value of 88% was obtained with 5% NaCl.

High Cr^{+6} ion concentration

A 500-ppm chromium solution was considered. The final concentration of chromium ions as a function of the number of cycles in the column with resin plus HCl was 0.08 ppm over 2 cycles, whereas in the resin with NaCl, the final concentration was 150 ppm over 10 cycles. The number of cycles indicated the number of times that the solution was passed through the column to eliminate the chromate ions; bear in mind that a competing action existed between the CrO_4^{-2} ions and the Cl^{-1} counterions. In the column containing HCl, two cycles were necessary, but the regeneration time required was longer. On the other hand, the column containing NaCl over 10 cycles

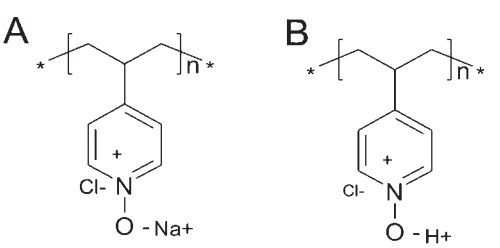

Figure 8 Proposed structures for the activation of RI10 with (a) NaCl and (b) HCl.

removed only 70% of Cr^{+6}. The chromate ion removal capability of the column treated with HCl was 99.8%.

To explain the observed behavior of Cr^{+6} ion exchange with HCl present at high Cr^{+6} ion concentrations, it was necessary to examine the ion-exchange mechanisms. As discussed, the stability diagram of the Cr^{+6}–H_2O system suggested that at low pH values, acid chromate ions ($HCrO_4^-$) were the dominant species and followed an equivalent sorption mechanism already discussed at low concentrations. The *N*-oxide groups of the resins produced here could not be protonated in the presence of hydrochloric acid, and this caused a high removal capability of chromium ions. It is known that the pH level is one of the most important factors influencing the adsorption behavior of metal ions on the resin. In fact, pH influences the formation of metal ions, the interaction of sorbent ions, and the surface structure of the sorbents.[32]

Previous studies[32] have pointed out that the ion-exchange kinetics of metal ions by chelating resins show an initial sharp decrease in the concentration of metal ions, followed by a more gentle variation, and finally, a leveling off. Initially, specific ions are adsorbed when a mixed solution of metal ions is present. The results presented in this study confirm such trends.

One of the aims of this study was the production of versatile resins that could have a dual cationic or anionic character. As compared to macroporous resins, those resins prepared here were not too expensive. Macroporous SBA resins with a quaternary functionality [$R—N^+—(CH_3)_3$] and polymer matrices of either polystyrene DVB or polyacrylic DVB are usually very expensive ($60–$170/kg of resin).[45] Studies have been reported on the use of SBA exchangers based on cellulose and lignocellulosic matrices for the efficient removal of Cr(VI) and other toxic anions, with costs ranging about one third of the polystyrene DVB or polyacrylic DVB resin cost. Less costly natural materials for toxic ion removal are available. Raw material used in another study, sawdust, is available from the timber industry as waste.[45] Alternatively, the relative cost of the materials synthesized here was lower than that of St–DVB ion exchangers and more than that of synthetic polymer-based materials. Because of their potential applications and relatively low cost, this study is currently being extended to other metals such as arsenic^{+3}, mercury^{+2}, copper^{+2}, and chromium^{+3}, where complex formation has been observed with the *N*-oxide group.[38]

CONCLUSIONS

Gel-type functionalized resins with excellent capabilities for chromate ion sorption were produced. The resin behavior depended on the morphology and amount of ionic groups. The protonated *N*-oxide group appeared to be the most efficient for chromate sorption, but it was not more efficient to regenerate. The ion-exchange resin could be used for 10 consecutive cycles without regeneration and achieved an overall removal efficiency of 95% with 4 ppm. At high chromate ion concentrations (500 ppm), it was possible to eliminate 99% of the chromate ions over 2 cycles in HCl solutions.

References

1. Ecatina, S.; Ecatina, A.; Axente, D.; Marcu, C. J Polym Sci Part A: Polym Chem 2004, 42, 2451.
2. Ratna, D.; Dalvi, V.; Deb, P. C.; Chakraborty, B. C. J Polym Sci Part A: Polym Chem 2003, 41, 2166.
3. Dragan, S.; Dinu, M. V.; Vlad, C. D. J Appl Polym Sci 2003, 89, 2701.
4. Forstner, U.; Wittmann, G. T. W. Metal Pollution in the Aquatic Environment; Springer-Verlag: Berlin, 1983.
5. Edwards, J. D. Industrial Wastewater Treatment; CRC/Lewis: Boca Raton, FL, 1995.
6. Fraser, B. G.; Pritzker, M. D. Sep Sci Technol 1994, 229, 2097.
7. Petruzzelli, D.; Tiravanti, G. Ind Eng Cem Res 1995, 34, 2612.
8. Arslan, M.; Yiğitoğlu, M.; Soysal, A. J Appl Polym Sci 2006, 101, 2865.
9. Gupta, V. K.; Imran, A. J Colloid Interface Sci 2004, 271, 321.
10. Kimbrough, D. E.; Cohen, Y.; Winer, A. M.; Creelman, L.; Mabuni, C. A. Environ Sci Technol 1999, 29, 1.
11. Gupta, V. K.; Gupta, M.; Sharma, S. Water Res 2001, 35, 1125.
12. Soo-Jin, P.; Young-Mi, K. J Colloid Interface Sci 2004, 278, 276.
13. Kobya, M. Bioresour Technol 2004, 91, 317.
14. Sandhya, B.; Tonni, A. K. Chemosphere 2004, 54, 951.
15. Auki, S. K.; Neufeld, R. D. J Chem Tech Biotechonol 1997, 70, 3.
16. Singh V. K.; Tiwari, P. N. J Chem Tech Biotechonol 1997, 69, 376.
17. Donghee, P.; Yeoung-Sang, Y.; Jong, M. P. Process Biochem 2005, 40, 2559.
18. Donghee, P.; Yeoung-Sang, Y.; Ji, H. J.; Jong, M. P. Water Res 2005, 39, 533.
19. Yoshio, N.; Kenji, T.; Toshiro, T. Water Res 2001, 35, 496.
20. Ruotolo, L. A. M.; Gubulin, J. C. React Funct Polym 2005, 62, 141.
21. Raji, C.; Anirudhan, T. S. Water Res 1998, 32, 3772.
22. Deng, S.; Bai, R. Water Res 2004, 38, 2424.
23. Gang, D.; Banerji, S. K.; Clevenger, T. E. Ind Eng Chem Res 2001, 40, 1200.
24. Chandat, M.; Rempel, G. L. Ind Eng Chem Res 1993, 32, 726.
25. Yigitoglu, M.; Arslon, M. Polym Bull 2005, 55, 259.
26. Bajpai, J.; Shrivastava, R.; Bajpai, A. K. Colloids Surf A 2004, 236, 81.
27. Bai, R. S.; Abraham, T. E. Bioresour Technol 2003, 87, 17.
28. Wang, C. C.; Chen, C. Y.; Chang, C. Y. J Appl Polym Sci 2002, 84, 1353.
29. Rivas, I. B.; Pooley, S. A.; Maturana, A. H.; Villegas, S. J Appl Polym Sci 2001, 80, 2123.
30. Neagu, V.; Bunia, I.; Plesca, I.; Popa, M. J Appl Polym Sci 2003, 88, 2956.
31. Paradhan, J.; Das, S. N.; Thakur, R. S. J Colloid Interface Sci 1999, 217, 137.
32. Lin, H.; Kimura, M.; Hanabusa, K.; Shirai, H.; Ueno, N.; Mori, Y. J Appl Polym Sci 2002, 85, 1378.
33. Sherrington, D. C. Chem Commun 1998, 2275.

34. Ortíz-Palacios, J.; Cardoso, J.; Manero, O. J Appl Polym Sci, to appear.
35. Rivas, B. L.; Maturana, H. A.; Peric, I. M. Polym Bull 1994, 33, 195.
36. Kolarz, B. N.; Jezierska, J.; Bartkouriak, D.; Gontarczyk, A. React Polym 1994, 23, 53.
37. Youssif, S. Arkivoc 2001, 249.
38. Anleu, E.; Cardoso, J.; Manero, O. J Appl Polym Sci 2002, 89, 1.
39. Herrmann, M. S. J Chem Educ 1994, 71, 323.
40. Colthup, N. B.; Daly, L. H. In Introduction to Infrared and Raman Spectroscopy; Wiberley, S. E., Ed.; Academic: New York, 1990; p 283.
41. Lin-Vien, D.; Colthup, N. B.; Fateley, W. G.; Grasselli, J. G. The Handbook of Infrared and Raman Characteristic Frequencies of Organic Molecules; Academic: New York, 1991; p 448.
42. Monroy-Soto, V. M.; Galin, J. C. Polymer 1984, 25, 254.
43. Hernández, M. A.; Velasco, J. A.; Rojas, F.; Lara, V. H.; Salgado, M. A.; Tamariz, V. Rev Int Contam Ambient 2003, 19, 183.
44. Gregg, S. J.; Sing, K. S. W. Adsorption, Surface Area and Porosity, 2nd ed.; Academic: New York, 1991; p 4.
45. Unnithan, M. R.; Anirudhan, T. S. Ind Eng Chem Res 2001, 40, 12.